A Latitude Survey of the Night Airglow

T. N. Davis*
Geophysical Institute, University of Alaska
College, Alaska

and

L. L. Smith
Fritz Peak Observatory, National Bureau of Standards
Boulder, Colorado

N65 32163

FACILITY FORM 602

29 (PAGES)

TMX54815 (NASA CR OR TMX OR AD NUMBER)

(THRU) 1

(CODE) 13

(CATEGORY)

GPO PRICE $ _____

CSFTI PRICE(S) $ _____

Hard copy (HC) 2.00

Microfiche (MF) .50

ff 653 July 65

*Now at Goddard Space Flight Center, Greenbelt, Maryland

ABSTRACT

32163

A four-color turret photometer has been used for shipboard observations of the night airglow and the aurora. Zenith observations have been obtained during 1962 close to the 70°W meridian from the northern auroral zone to the Antarctic pack ice. Most of the observations were taken during the Southern Winter.

Maximums in the [OI] 5577A intensity were found near 30-40°N and 40°S, with the Southern Hemisphere level being generally lower than that in the Northern Hemisphere. The [OI] 6300A latitudinal variation was similar to that of [OI] 5577A except that maximums in the latitudinal distribution were found near 15° geomagnetic north and south latitudes. In contrast with the the [OI] emissions, the sodium group (NaD doublet and OH bands near 5893A) generally increased to the south with maximums near 20-30°N and 40-50°S geographic latitude. The total 5340A background increased from north to south. When the integrated starlight and zodiacal light components were subtracted from the total background, the resultant terrestrial component showed a pronounced minimum at low latitudes and apparent symmetry about the geomagnetic equator.

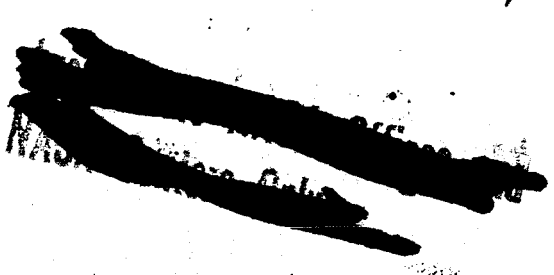

I. Introduction

Photometric observations of the aurora and the night airglow were made aboard the U.S.N.S. Eltanin during the period March - November, 1962. The Eltanin departed from New York in late March and moved northward into the Laborador Sea where photometric observations of aurora were made on four nights. After returning to New York, the Eltanin departed on May 24 on a trip southward and arrived in Valparaiso, Chile on June 27. Clear skies existed throughout most of this cruise and useful airglow observations were obtained on 17 nights. In the period July - November 1962, the Eltanin made several cruises southward from Valparaiso and useful observations (during clear, moonless dark hours) were obtained on 36 nights. See Figure 1 for the positions of the Eltanin when the observations were made.

Observations were made in four narrow wavelength bands centered near 5577, 6300, 5893 and 5340A with a turret photometer built by the Fritz Peak Observatory following a design by Purdy, Megill and Roach (1961). This instrument has a 5° diameter circular field of view and was mounted on a free swinging gimbal to assure observation of the zenith. The gimbal mount was effective in reducing the effect of the ship's motion to the extent that the photometer axis pointed to within 5° of the zenith throughout most of the observations. Observations at a given wavelength were obtained at 5 minute intervals.

The two-color method (Roach and Meinel, 1955) was applied to the 5577, 6300 and 5893A observations in an attempt to remove the contributions due to airglow continuum, zodiacal light, and integrated starlight; the method involves subtraction of these contributions as determined by observation through the 5340A filter. Details of the data reduction and calibration procedures together with tabulations of the results are given in a limited circulation report (Davis and Smith, 1964).

II. Results

Several types of variation occur in the night airglow; these types include latitudinal variation, seasonal variation, diurnal variation, nightly variation and possibly also effects produced by high-altitude explosions. Considering the nature of the data taken so far aboard the Eltanin, it is impossible to completely separate the different types of variation. An additional complication arises from inhomogenieties of the data, since on some nights complete observations are obtained, while on others, as little as only an hour of observation may be available.

II. A. Variation of [OI] 5577A

A. 1 Night-to-night and Diurnal Variations

The observations show two categories of diurnal variation in 5577A. One type, illustrated in Figure 3A, is one in which little variation in the 5577A intensity occurs during the middle of the night. In the second category are those nights in which an enhancement occurs during some part of the night; see Figures 3B and 3C. Evidently the time at which the enhancement occurs is random, since averaging over a number of nights (Figure 4A) yields a nearly constant level of 5577A emission throughout the night. The data do not indicate any latitude dependence of the character of the diurnal variation, although the quantity of data is not sufficient to rule out such a dependence.

A. 2 Latitude and Seasonal Variations

Figure 5A shows a plot of the nightly average and nightly range of hourly averages of 5577A intensity versus date. The variations here are of several types: latitude, nightly, and seasonal. The same data are plotted in Figure 5B against latitude and those taken during a limited period, May 24 - September 1, 1962, are plotted similarly in Figure 5C. An attempt to eliminate part of the nightly variation is shown in Figure 5D, which is compiled by taking the averages of all data in 10 latitude-degree groups. Figures 5C and 5D provide

A complication to the determination of the intensities of the [OI] 5577, [OI] 6300 and NaD 5893A emissions arises due to contamination from nearby OH band emissions. Figure 2 shows the filter transmission characteristics and wavelengths of the [OI]and NaD (doublet) emissions. A correction to the [OI] 5577A intensity is required due to the presence of the OH(7-1) band emissions with the band head at 5562A. Using estimates of the mean zenith intensities of the OH 5562A band and [OI]5577A line emissions given by Roach (1956), 15R and 250R, respectively, or measurements by Krassovsky, Shefov, and Yarin (1962) together with the known transmission characteristics of the 5577A filter, it is estimated that on the average approximately 90% of the intensity remaining after correction for continuum sources is due to the [OI] 5577A emission. Although the 6300A filter is quite narrow, contamination from the OH (9-3) band with band head near 6256A is significant. Based on data given by Chamberlain (1961, pp. 555-557) the OH contribution through the 6300A filter is estimated to be in the neighborhood of 10 to 20 Rayleighs. At the low levels of [OI] 6300A emission encountered during some of the measurements described below, the OH contamination is especially severe. Serious contamination also occurs through the 5893A filter as a result of the OH (8-2) band near 5886A. The NaD and OH emissions can covary (see Chamberlain, 1961 p. 517) and it is estimated that approximately 70% of the line and band emission measured through the 5893A filter is due to the NaD doublet at 5890-5896A. Since the observations reported here are obtained over a wide range of latitude, it must be recognized that there is much uncertainty about the OH contributions. Hence, no attempt has been made to correct the results presented below for OH contamination.

the best indication of both the seasonal and latitude variation in 5577A intensity. The northern hemisphere data are obtained over a short period of time (May 24-June 2) and therefore include only diurnal, nightly and latitudinal variations. These types of variation cannot be separated completely, however Figures 5C and 5D indicate the possibility of a latitudinal maximum near 30-40° geographical latitude and decreasing intensity as the equator is approached. Moving southward from the equator, there is some increase in the average intensities (Figures 5C and 5D) with a weak maximum occurring near geographic latitude 40°. There appears to be a definite decrease in the 5577A airglow level to the south as far as 65° geographic latitude where the observations end. The data are consistent with a seasonal variation in which there is a maximum in summer and minimum in winter.

II. B. Variation of [OI] 6300A

B. 1 Night-to-night and Diurnal Variations

Unlike [OI]5577A, the [OI] 6300A emmission shows a definite variation through the night. The well-known post-twilight decay and the lesser predawn increase are evident in the data taken at all latitudes; see Figure 4B. A nightly variation occurs in [OI] 6300A; for the most part it appears as an over-all change in the level of the emission through the night.

The only exception occured when the Eltanin was near the equator. On the two nights shown in Figure 6, and possibly on a third, an enhancement in [OI] 6300A developed in the hours near midnight. These monochromatic enhancements may be related to the intertropical red arcs described by Barbier, Weill, and Glaume (1961); however, the enhancement is relatively small and apparently restricted in time to the hours near local midmight. Although the midnight enhancements observed on June 2 and 6, 1962 may not be related to the intertropical red arcs, the zones where the intertropical red arcs appear coincide with the positions of the two maxima on the curve of Figure 7C. There is much

similarity between the observed latitudinal distribution of 6300A in the region within 30°N and 30°S magnetic latitude and the F region electron content per vertical column calculated by Duncan (1960). In this calculation, he assumed an initially uniform electron distribution to be modified by electrodynamic lift and subsequent settling down the geomagnetic field lines. Since it has been found that the intensity of the 6300A emission is approximately proportional to the maximum electron density in the F2 region (Huruhata et al., 1959), it appears possible that the processes decribed by Duncan may contribute to the observed 6300A distribution in the tropic regions.

B. 2 Seasonal and Latitudinal Variation

The diagrams showing all data versus latitude (Figure 7A), Southern Hemisphere Winter versus latitude (Figure 7B) and 10-latitude-degree averages (Figure 7C) show generally higher intensities in the Northern Hemisphere and thus may indicate a seasonal variation of [OI] 6300A similar to that of [OI] 5577A; namely, a maximum in summer and minimum in winter. Maximums in the latitudinal distribution of intensity appear near the equator at approximately 15°N and 15°S geomagnetic latitude.

Another representation of the [OI]6300A data is shown in Figure 8, where the observations are plotted against latitude and local time and then used to compile isophotes of zenith intensity. This diagram is suggested by a similar one by Barbier (1961) and should be compared with it.

The intensity ratio 6300A/5577A obtained from individual airglow observations is highly variable; ratios averaged over a night's observations range between 0.09 and 0.67. The average ratio of the observations in the region 30-60°S is 0.25.

II. C. Variation of the NaD group

As mentioned previously, the 5893A filter passes both the NaD doublet centered near 5893A and OH emissions including the OH (8-2) emission at 5886A.

These emissions will be referred to here as the sodium group. The sodium group intensity remains relatively constant on a given night, and the average diurnal variation curves, Figure 4C, indicate little or no regular variation through the night.

Plots of the sodium group variations versus latitude (Figure 9), show a trend toward higher intensities going from north to south. Superimposed on this trend are irregularities; a maximum appears near 20-30°N, and there is a minimum centered near 0-10°N. Another maximum may exist near 10-20°S, and relatively high intensities are observed over the latitude range 30-57°S. The intensities observed between 58 and 65°S are relatively low. Overall, the variation with latitude of the sodium group intensity is somewhat less than that of the [OI] 5577A and 6300A emissions. The observed sodium group intensities are consistent with a seasonal variation in which there is a maximum in winter and minimum in summer.

II. D. Variation of the Background near 5340A

Except for some evening twilight contamination or post-twilight enhancement, the background near 5340A averaged over all data remained relatively constant through the night; see Figure 4D. The total background near 5340A, shows a general increase from north to south. This total background includes components from integrated starlight, zodiacal light and airglow continuum. Using integrated starlight intensities given by Roach and Megill (1961) and zodiacal light intensities from Roach and Smith (manuscript in preparation) the contribution of these components to the total background is determined and displayed in Figure 10. The background component due to airglow continuum is obtained by subtraction and is also shown in Figure 10. The airglow continuum determined by this method shows a pronounced minimum at low latitudes and appears to be fairly symmetrical

about the geomagnetic equator. For comparison, one-year average values of the airglow continuum obtained by Roach and Smith for two airglow observatories, Fritz Peak, Colorado and Haleakala, Hawaii, are indicated on Figure 10 by the numbers 1 and 2, respectively.

II. E. Auroral Zone Observations

Limited observations of auroras were made during March and April 1962 at the northern auroral zone, however high seas and partial cloudiness during the period of these observations detract from their value. Bright auroral forms were observed in the zenith during part of the observations; 5577A intensities ranged up to 92kR, those of 6300A ranged up to 1.8kR. Although the results may not be meaningful, intensities of the sodium group were not much greater than that observed in the airglow (see Figure 7).

One interesting aspect of the auroral observations is the behavior of the average [OI] 6300/5577 ratio. Individual values of the ratio varied between 0.007 and 0.5, with the ratio decreasing with increasing 5577A and 6300A intensity: see Figure 11. The higher values of the ratio tend to occur in the hours before midnight, and the lower values after midnight. The tendency for the 6300A/5577A ratio to decrease with increasing 5577A intensity may be due to electron deactivation of the oxygen ^1D level in the brighter auroras (Chamberlain 1961, p. 315). Also, molecular deactivation of the ^1D level by collisions with O_2 may be responsible for the results shown in Figure 12 if the brightening of 5577A is associated with increasing auroral exitation at low altitude in the post-midnight hours.

III Summary and Discussion of Results

While it is not possible to separate completely the types of variations which influence the results obtained here, these results are compatible with

the diurnal, seasonal, and latitudinal variations shown in Table I in summary form. As indicated in the right-hand column of Table I, the observations may be interpreted as suggesting either a rather general seasonal variation or a pronounced hemispherical effect. One aspect of the observations which is evident in the various diagrams but which is not indicated in Table I is the sizable nightly variation observed in each of the airglow components. A comparison of these nightly variations with the global magnetic activity index Kp did not reveal any connection. However, it is interesting that the results of this study do suggest that the latitudinal distribution of intensity of some airglow emissions may be influenced by the configuration of the geomagnetic field.

The diurnal and nightly variation of 5577A observed on the Eltanin in 1962 is somewhat less than that observed in previous years on the Soya (Nakamura, 1957 and 1959). Assuming that the calibrations are correct for each set of data, the Eltanin observations show lower absolute 5577A intensities as well. Two differences exist in the conditions under which these sets of data were obtained: the observation aboard the Soya were made during southern summer and during a period of high solar activity whereas the Eltanin observations were made near a minimum in the solar cycle and during southern winter.

Several factors affect the accuracy of the results reported here. One is the uncertainty in the absolute calibration of the comparison source. Another is the problem of OH contamination, which is discussed above. Since the observed 5577A intensities in the southern hemisphere are low, somewhat more than 10% of the 5577A intensities reported here may be due to OH. If it is assumed that the NaD and OH emissions co-vary, then, at all times, approximately 70% of the sodium group intensity observed through the 5893A filter is due to NaD 5893A.

It has been found during these observations that the 2-color method is not a completely satisfactory means of eliminating the astronomical and airglow continuum components from the observations. In using that method it has been assumed that a single proportionality constant relating the contaminants to the 5340A intensity is applicable at all observed light intensities. Observations made during periods of relative stability in the level of the various airglow emissions and in which the astronomical component varied (for example, passage of the Milky Way over the photometer)indicate that the proportionality constant for each wavelength was too low to correct for the astronomical component. On the other hand, if one adopts proportionality constants of sufficient size to give a complete correction when the astronomical components are large, an obvious over-correction occurs at other times (the line emission intensities become negative). Consequently, the 2-color method, as used here, must be considered as a very crude means of correction for the atmospheric continuum and astronomical backgrounds. Despite the various uncertainties which influence the absolute values of the emissions reported here, the trends summarized in Table I appear to be real in that they appear in the data prior to and after the application of any corrections.

Acknowledgements

We are grateful to Dr. Franklin E. Roach for his aid and advice throughout this study. Dr. Manfred H. Rees also has contributed many helpful discussions and several specific suggestions which we have followed. Most of the data presented here were collected through the conscientious shipboard efforts of Mr. F.T. Berkey. Part of the work was accomplished while one of us (T.N.D.) was a Guest Worker at the Fritz Peak Observatory of the National Bureau of Standards. This work was supported by the Office of Antarctic Programs of the National Science Foundation grant number 18704.

References

Barbier, D., Les variations d'intensité de la raie 6300A de la luminescence nocturne, Ann. Geophys., 17, 3-15, 1961.

Barbier, D., G. Weill, and J. Glaume, L'emission de la raie rouge du ciel nocturne en Afrique, Ann Geophys., 17, 305-318, 1961.

Chamberlain, J.W., Physics of the Aurora and Airglow, Academic Press, New York and London, pp. 315, 517, 555-557, 1961.

Davis, T.N., and L.L. Smith, Latitudinal and seasonal variations in the night airglow, Report No. UAG-R156, Geophysical Institute, College, Alaska, p. 19, 1964.

Duncan, R.A., The equatorial F-region of the ionospher, J. Atmos, Terr. Phys., 18, 89-100, 1960.

Huruhata, M., T. Nakamura, H. Tanabe, and T. Tohmatsu, Oxygen red line in the night airglow and ionospheric F2 region, Rept. Ionos. and Space Res. in Japan, 13, 283-289, 1959.

Krassovsky, V.I., N.N. Shefov, and V.I. Yarin, Atlas of the airglow spectrum 3000-12400Å, Planet. Space Sci., 9, 883-915, 1962.

Nakamura, Junji, Latitude effect of night airglow, J. Geophys. Res., 62, 487-488, 1957.

Nakamura, Junji, Latitude effect of night airglow, Rept. Ionosphere Res. in Japan, 12, 419-427, 1959.

Purdy, C.M., L.R. Megill, and F.E. Roach, A new airglow photometer, J.cf Research of the National Bureau of Standards, 65C, 213-216, 1961.

Roach, F.E., Manual for photometric observations of the airglow during the International Geophysical Year, NBS Rept. 5006, National Bureau of Standards, Boulder, Colorado, 1956.

References

Roach, F.E., and L.R. Megill, Integrated starlight over the sky, Astrophys. J., 133, 228, 1961.

Roach, F.E., and A.B. Meinel, The height of the nightglow by the Van Rhijn method, Astrophysical Journal, 122, 530-553, 1955.

TABLE TITLE

I Summary of Eltanin airglow observations.

Figure Titles

1. Location of the Eltanin on nights when useful night-time observations were made.
2. Transmission characteristics of the interference filters and locations of line emissions near the filter peaks.
3. A) Example of a night of relative quiet in the airglow variations (plot of hourly averages); B) and C) are examples of active variations in 5577A.
4. Average diurnal variation of the airglow emissions.
5. Nightly average and range of hourly average of 5577A: A) versus date, B) all data versus latitude, and C) for data taken May 24 to September 1, 1962. D) ten-degree latitude averages versus latitude, all data.
6. Nights on which enhancements in 6300A occurred.
7. Nightly average and range of hourly averages of 6300A: A) for all data and B) for data taken May 24 to September 1, 1962. C) ten-degree latitude averages versus latitude for all data.
8. Isophote map giving zenith intensity of 6300A in rayleighs as derived from the Eltanin observations during Southern Winter 1962. The dashed lines A-A' indicate possible arc-like zones of enhanced radiation. (Compare with Barbier, 1961)
9. Nightly average and range of hourly averages of the sodium group (NaD 5893A and OH): A) for all data and B) for observations taken May 24 to September 1, 1962. C) Ten-degree latitude averages versus latitude, all data.

Figure Titles (continued)

10. Ten-degree latitude averages of the 5340A background: A) total background, B) the component due to integrated starlight and zodiacal light as computed by Roach and Smith (private communication), and C) the airglow continuum component determined by subtracting curve B from curve A. The point labeled (a) represents the one-year average airglow continuum obtained by Roach and Smith for the Fritz Peak Observation (geographic latitude 40°, geomagnetic latitude 50°) and the points labeled (2) are the same for the Haleakala Observatory (geographic latitude 20°, geomagnetic latitude 10°).

11. The zenith intensity ratio 6300A/5577A plotted against the zenith intensity of 5577A in the auroral zone aurora.

Table I Summary of Eltanin Airglow Observations

Emission	Diurnal Variation	Latitudinal Variation	Seasonal Variation (or Hemispherical Difference)
[OI] λ5577	No regular diurnal variation irregular activity (sometimes monochromatic) on some nights.	Apparent maximum near 30-40°N, decreasing to minimum near equator, then gradual increase to maximum near 40°S. Decreasing intensity southward as far as 65°S.	Compatible with maximum in summer and minimum in winter. (Or if no such general seasonal variation, the intensties are greater in the northern hemisphere than in the southern hemisphere).
[OI] λ6300	Common post-twilight and predawn variations persist at all latitudes. Monochromatic enhancement observed at local midnight near equator.	Apparent maxima near 15° geomagnetic north and south.	
NaD+ OH near λ5893	No diurnal variation evident.	Apparent maximum near 20-30°N. Shallow minimum near 0-10°N. Irregular increase southward to maximum near 40-50°Sand, decreasing from 55°S to 65° south.	Compatible with minimum in summer and maximum in winter. (or, as above, higher relative intensity in the southern hemisphere).
Background near λ5340	Possible post-twilight enhancement, otherwise no regular diurnal variation.	Relatively steady increase of total background from 40°N to 65°S. Astronomical components maximize in equatorial region; airglow continuum lowest in equatorial region with apparent symmetry about geomagnetic equator.	

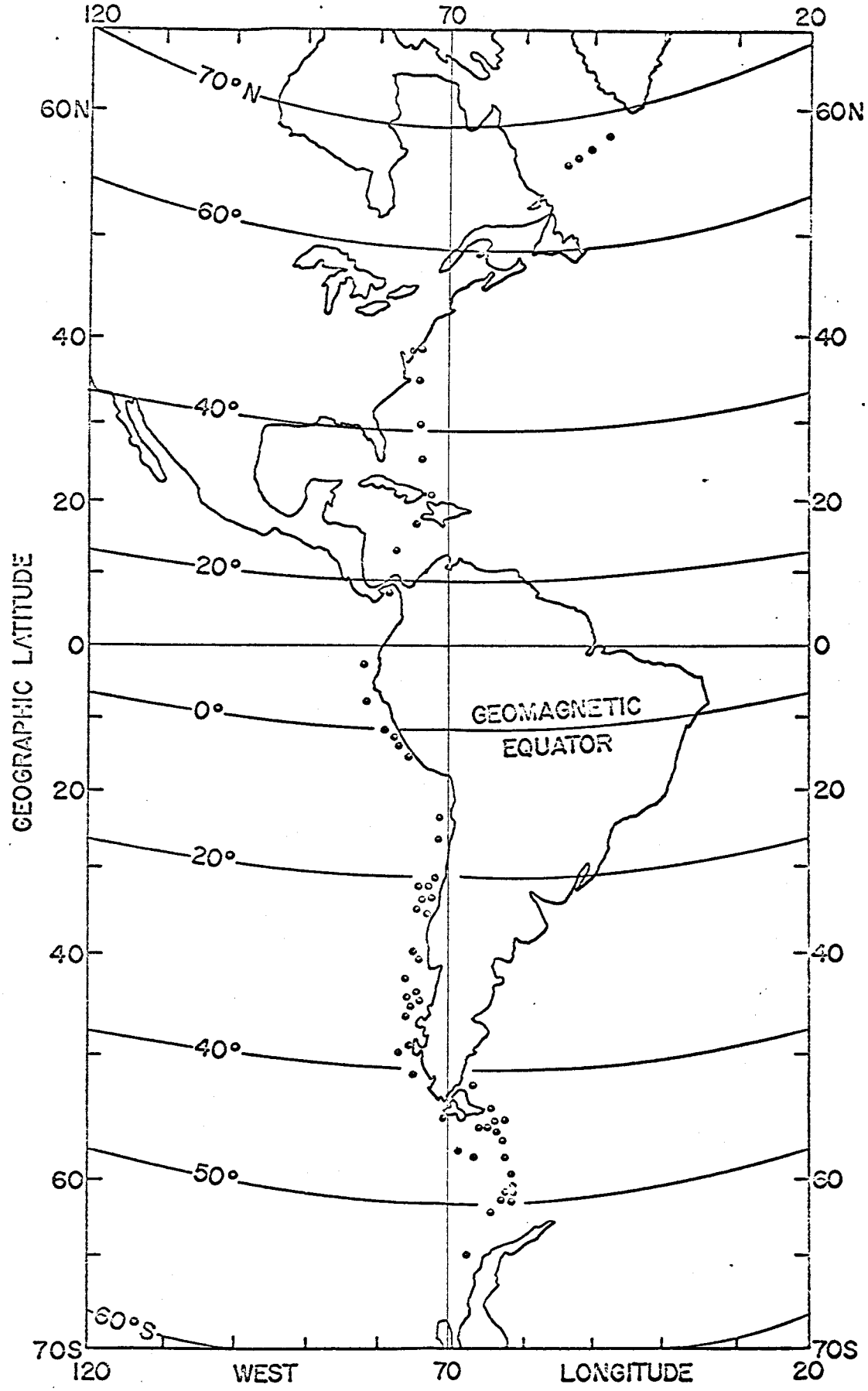
120
70
20
70°N
60N
60°
40
40°
20
20°
0
0°
GEOMAGNETIC
EQUATOR
20
20°
40
40°
60
50°
60°S
70S
120
WEST
70
LONGITUDE
20
GEOGRAPHIC LATITUDE

Figure 1

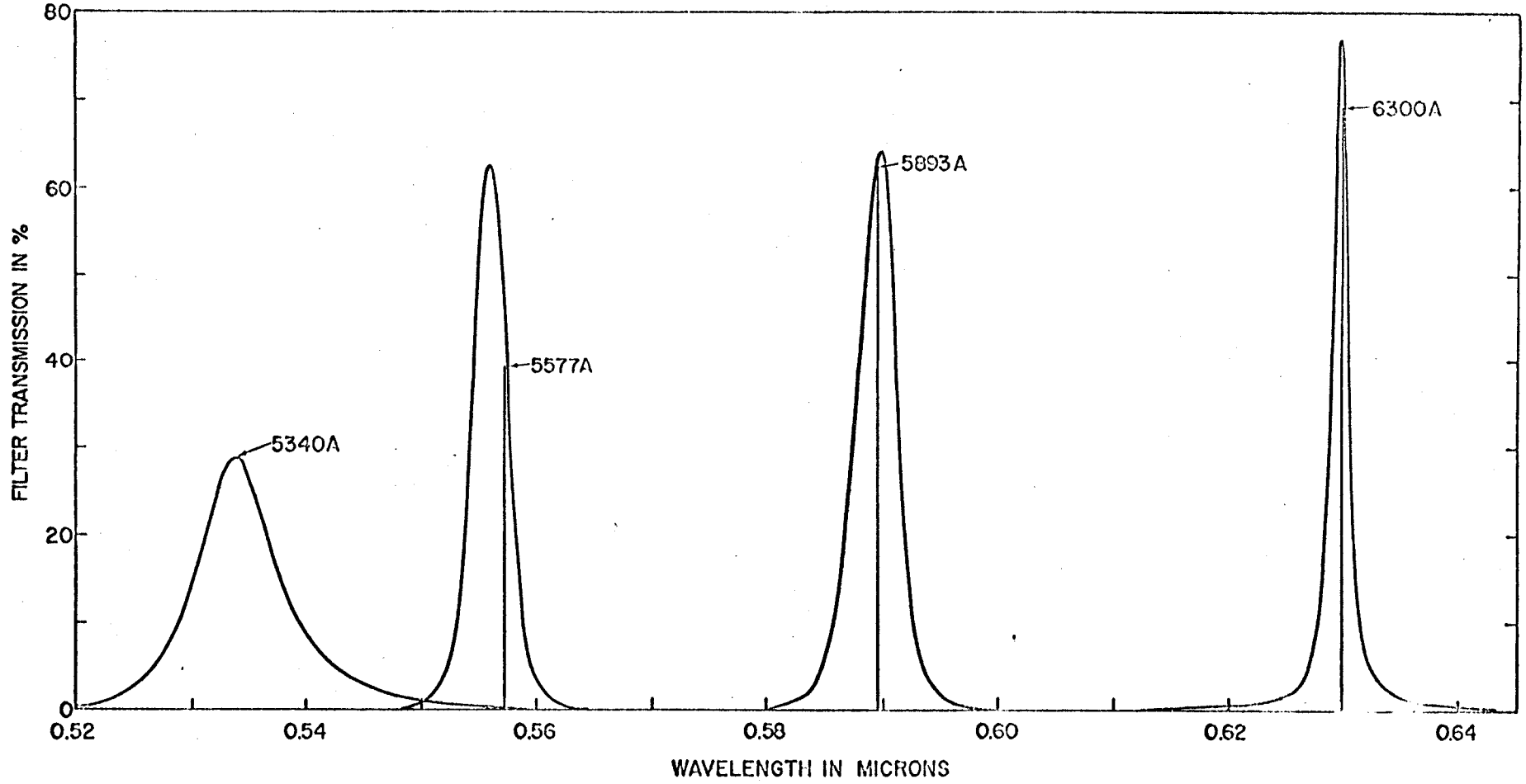
80
60
40
20
0
FILTER TRANSMISSION IN %
5340A
5577A
5893A
6300A
0.52
0.54
0.56
0.58
0.60
0.62
0.64
WAVELENGTH IN MICRONS

Figure 2

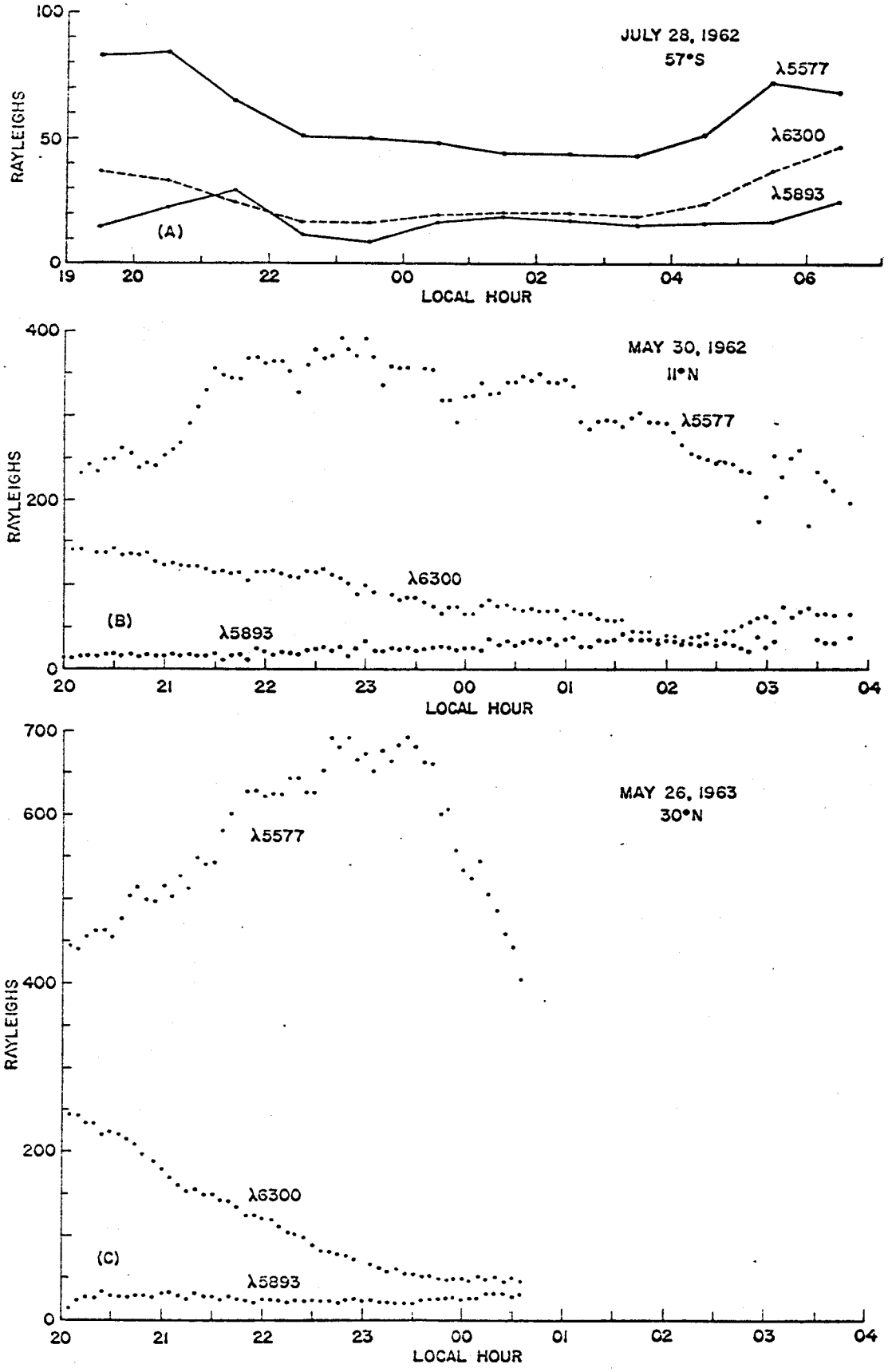
JULY 28, 1962
57°S
λ5577
λ6300
λ5893
(A)
RAYLEIGHS
LOCAL HOUR
MAY 30, 1962
11°N
λ5577
λ6300
λ5893
(B)
RAYLEIGHS
LOCAL HOUR
MAY 26, 1963
30°N
λ5577
λ6300
λ5893
(C)
RAYLEIGHS
LOCAL HOUR

Figure 3

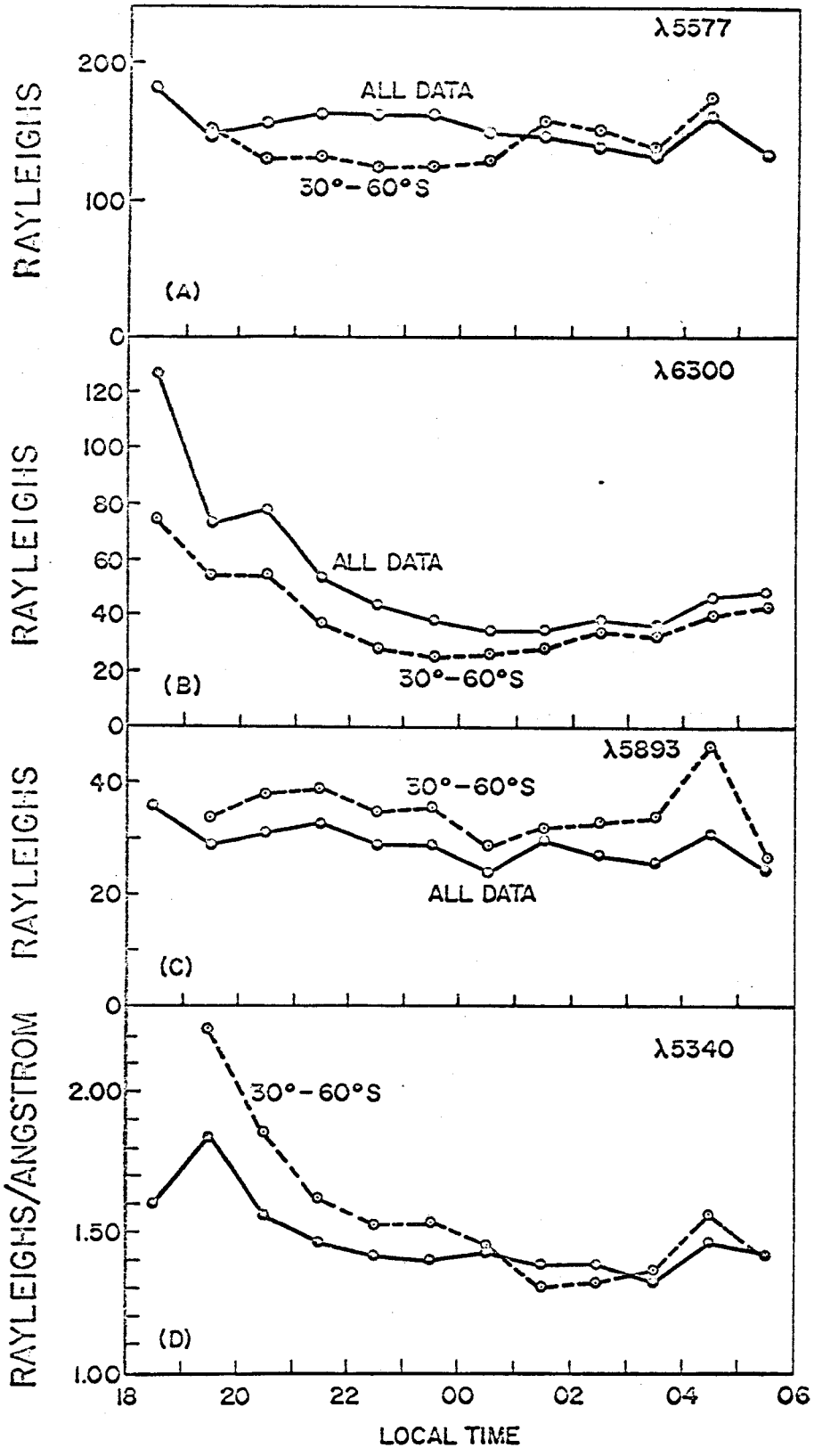
λ5577
ALL DATA
30°-60°S
(A)
RAYLEIGHS
200
100
0
λ6300
ALL DATA
30°-60°S
(B)
120
100
80
60
40
20
0
λ5893
30°-60°S
ALL DATA
(C)
40
20
0
λ5340
30°-60°S
(D)
RAYLEIGHS/ANGSTROM
2.00
1.50
1.00
18
20
22
00
02
04
06
LOCAL TIME

Figure 4

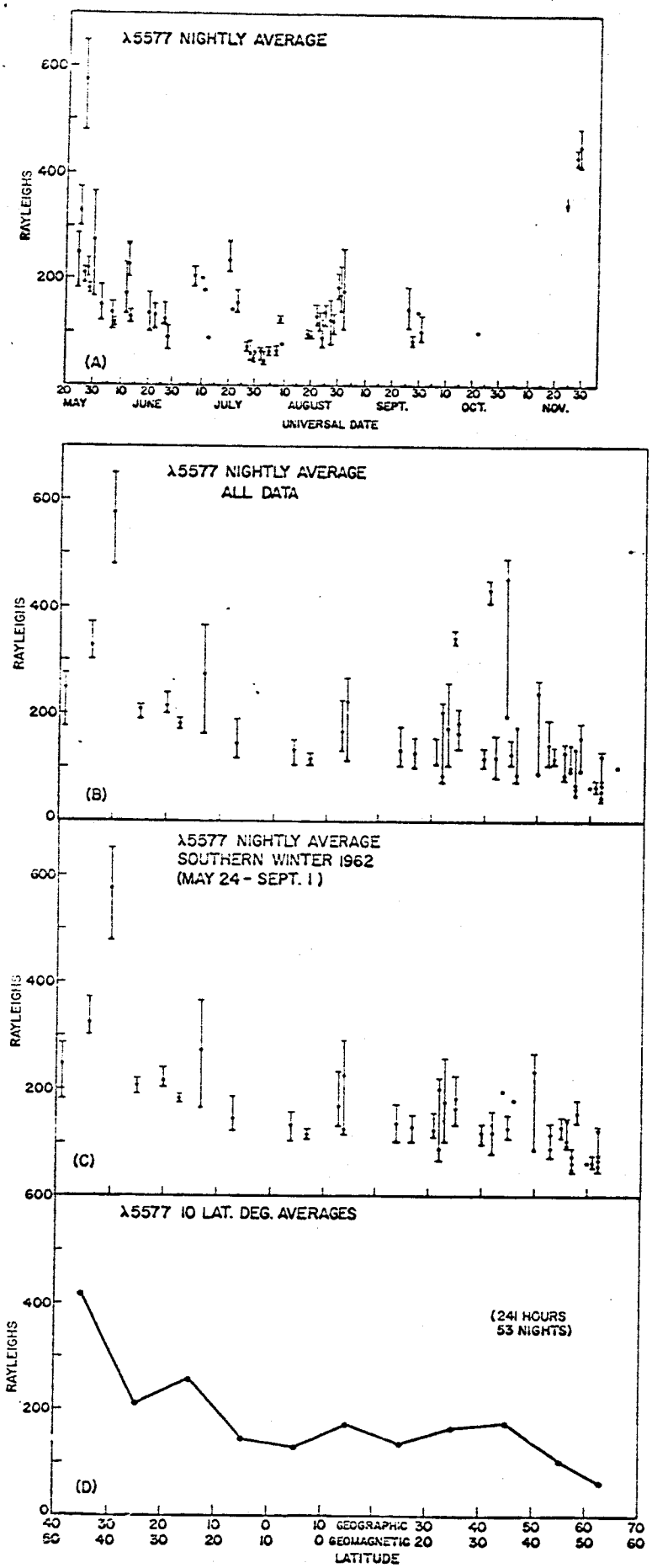
λ5577 NIGHTLY AVERAGE
RAYLEIGHS
600
400
200
(A)
20 30 10 20 30 10 20 30 10 20 30 10 20 30 10 20 30
MAY JUNE JULY AUGUST SEPT. OCT. NOV.
UNIVERSAL DATE
λ5577 NIGHTLY AVERAGE
ALL DATA
RAYLEIGHS
600
400
200
0
(B)
λ5577 NIGHTLY AVERAGE
SOUTHERN WINTER 1962
(MAY 24 - SEPT. 1)
RAYLEIGHS
600
400
200
(C)
λ5577 10 LAT. DEG. AVERAGES
RAYLEIGHS
400
200
0
(241 HOURS
53 NIGHTS)
(D)
40 30 20 10 0 10 GEOGRAPHIC 30 40 50 60 70
50 40 30 20 10 0 GEOMAGNETIC 20 30 40 50 60
LATITUDE

Figure 5

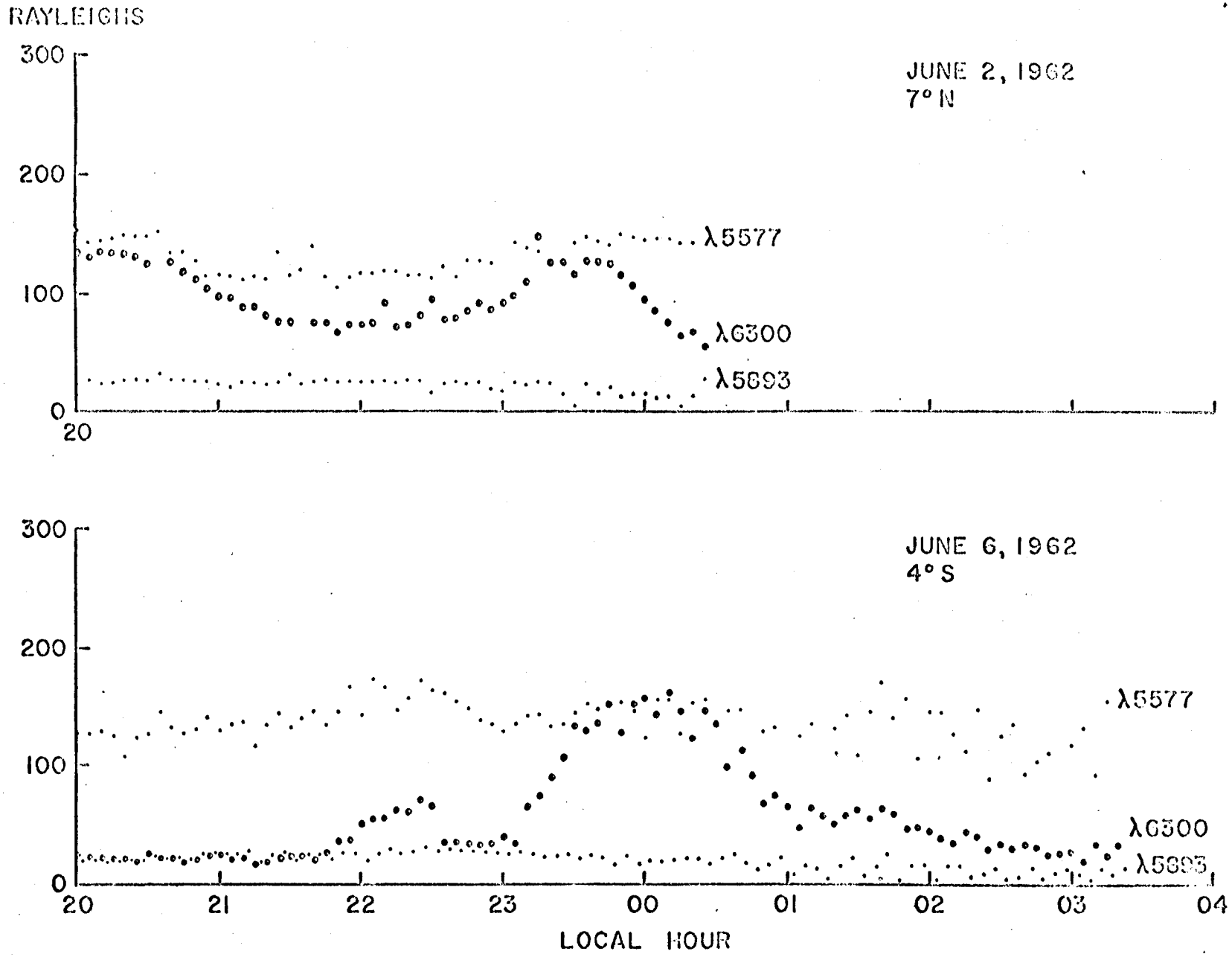
RAYLEIGHS
300
200
100
0
20
JUNE 2, 1962
7° N
λ5577
λ6300
λ5893
300
200
100
0
JUNE 6, 1962
4° S
λ5577
λ6300
λ5893
20
21
22
23
00
01
02
03
04
LOCAL HOUR

Figure 6

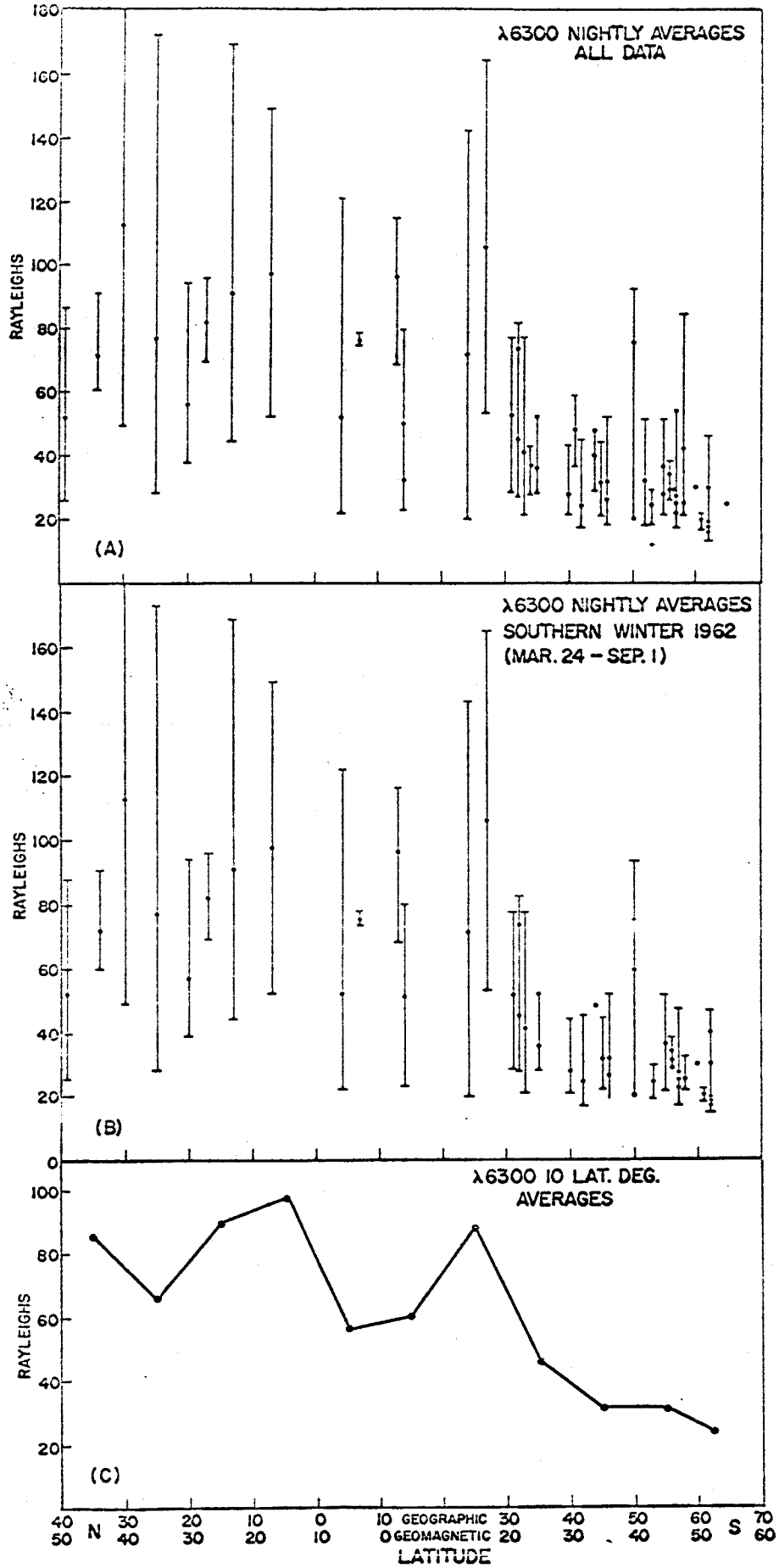
λ6300 NIGHTLY AVERAGES
ALL DATA
RAYLEIGHS
(A)
λ6300 NIGHTLY AVERAGES
SOUTHERN WINTER 1962
(MAR. 24 – SEP. 1)
RAYLEIGHS
(B)
λ6300 10 LAT. DEG.
AVERAGES
RAYLEIGHS
(C)
40 N 30 20 10 0 10 GEOGRAPHIC 30 40 50 60 S 70
50 40 30 20 10 0 GEOMAGNETIC 20 30 40 50 60
LATITUDE

Figure 7

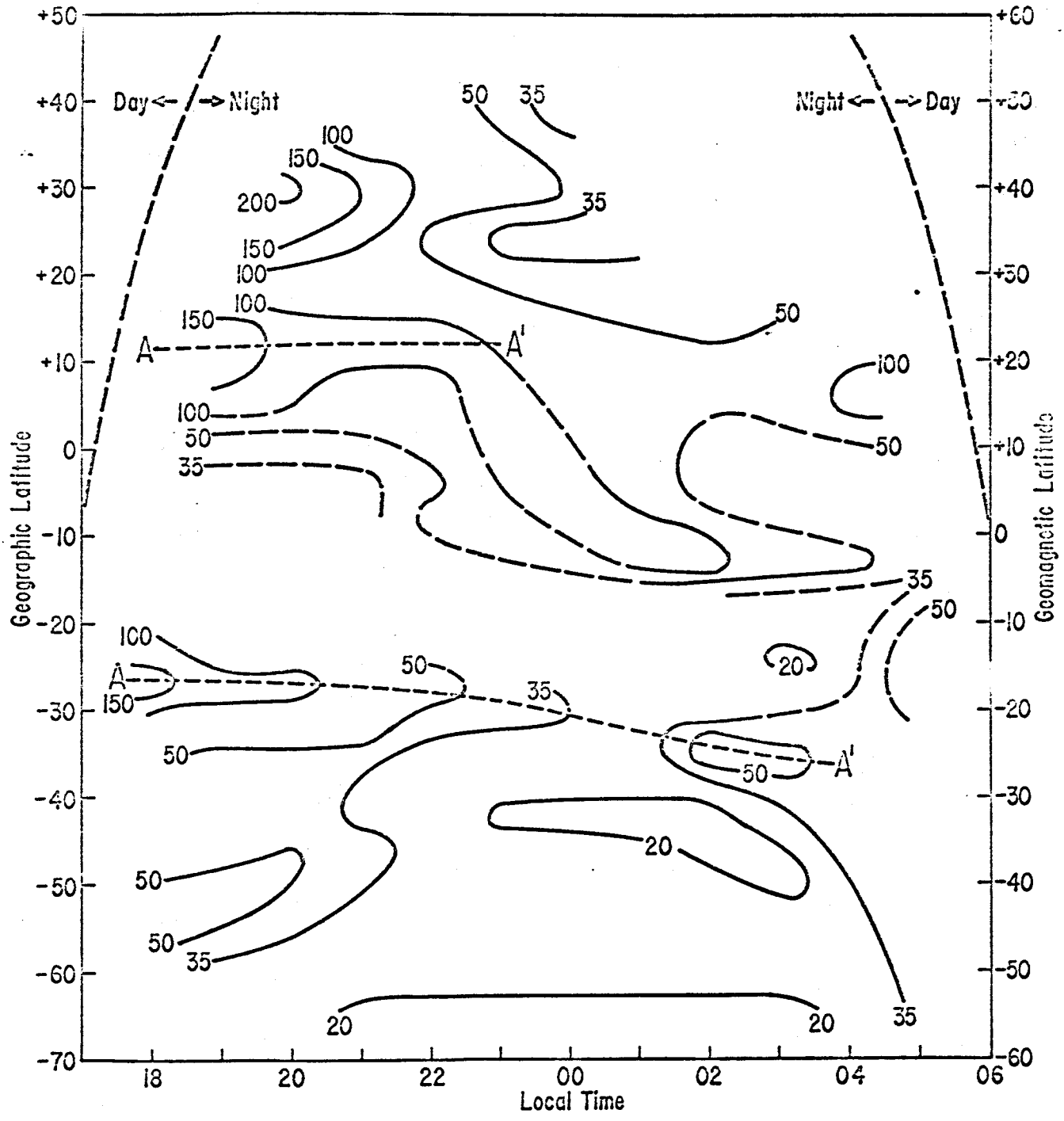
+50
+40
+30
+20
+10
0
-10
-20
-30
-40
-50
-60
-70
+60
+40
+30
+20
+10
0
-10
-20
-30
-40
-50
-60
Day <- -> Night
Night <- -> Day
Geographic Latitude
Geomagnetic Latitude
18
20
22
00
02
04
06
Local Time
A
A'
100
150
200
50
35
20

Figure 8

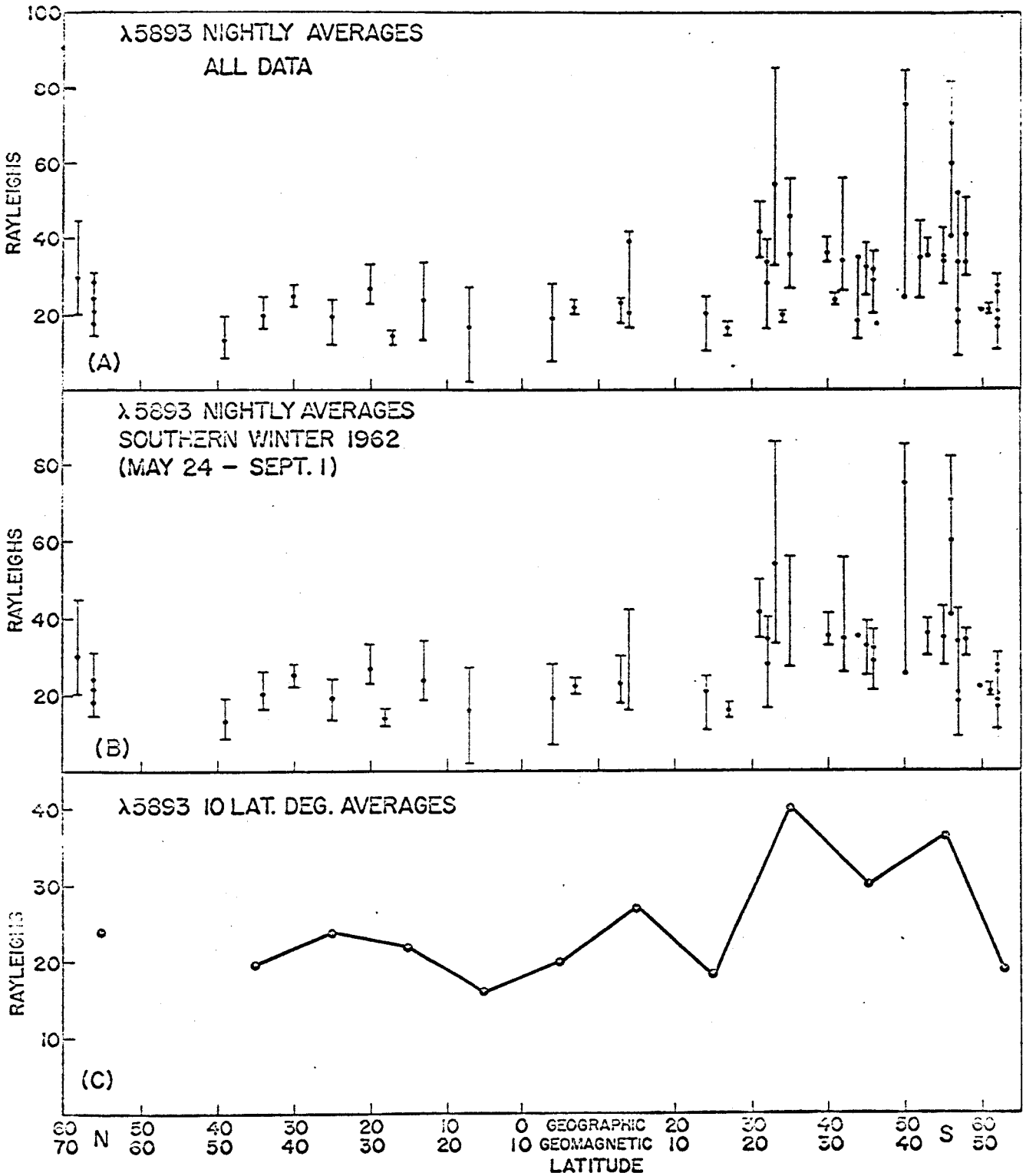
λ5893 NIGHTLY AVERAGES
ALL DATA
RAYLEIGHS
(A)
λ5893 NIGHTLY AVERAGES
SOUTHERN WINTER 1962
(MAY 24 – SEPT. 1)
RAYLEIGHS
(B)
λ5893 10 LAT. DEG. AVERAGES
RAYLEIGHS
(C)
GEOGRAPHIC
GEOMAGNETIC
LATITUDE
N
S

Figure 9

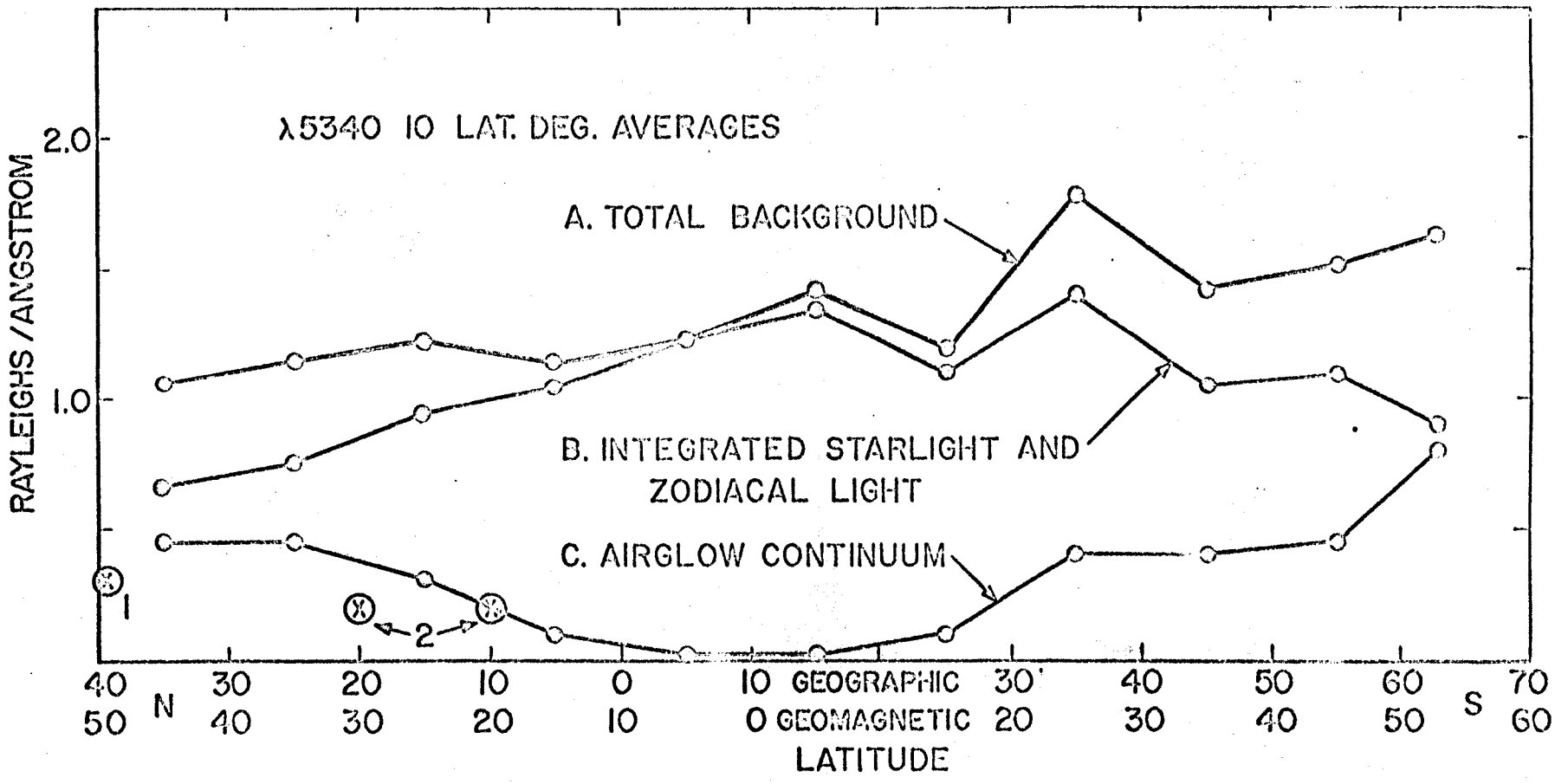
λ5340 10 LAT. DEG. AVERAGES
RAYLEIGHS /ANGSTROM
2.0
1.0
A. TOTAL BACKGROUND
B. INTEGRATED STARLIGHT AND
ZODIACAL LIGHT
C. AIRGLOW CONTINUUM
1
2
40 30 20 10 0 10 GEOGRAPHIC 30 40 50 60 70
50 N 40 30 20 10 0 GEOMAGNETIC 20 30 40 50 S 60
LATITUDE

Figure 10

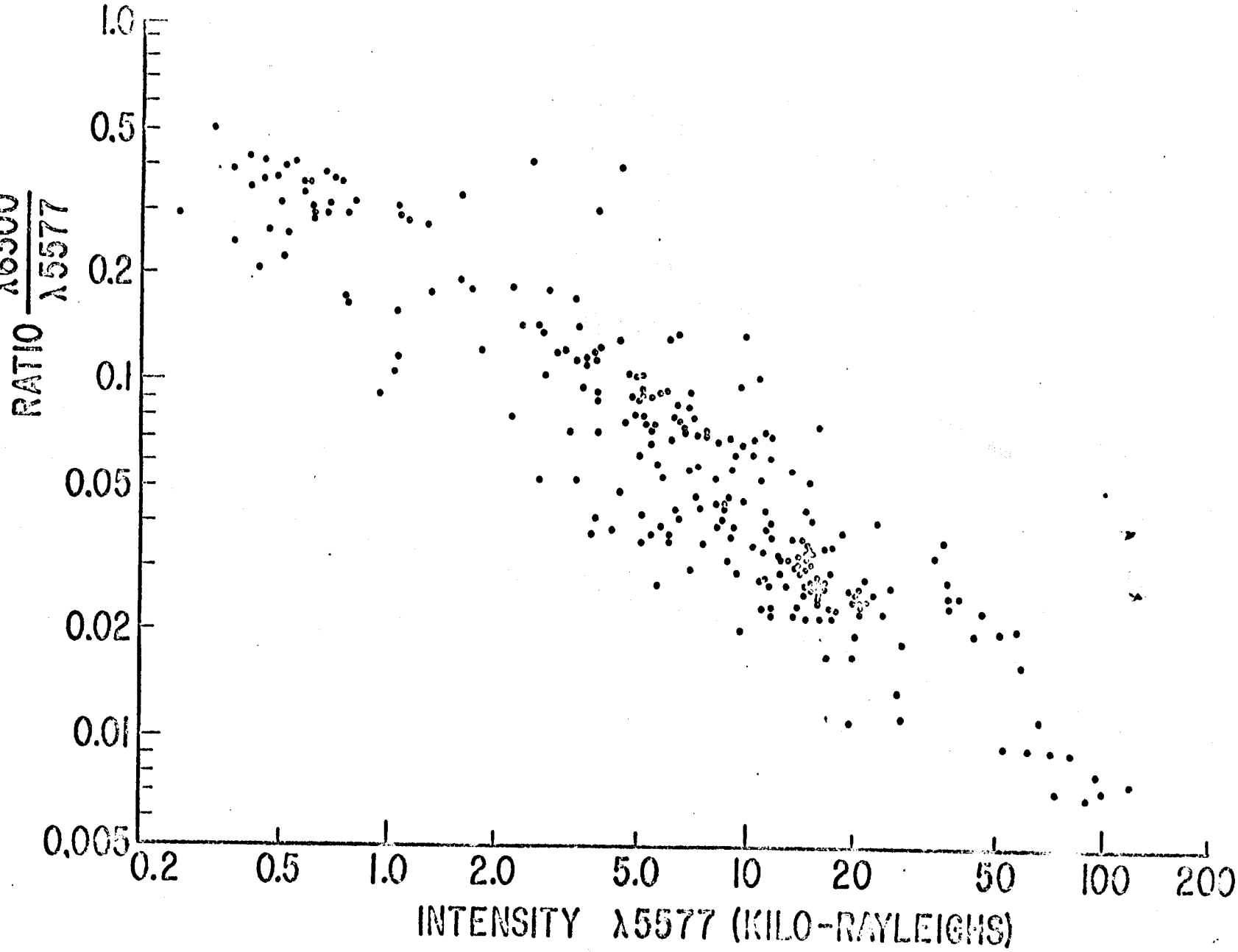
RATIO λ6300/λ5577
1.0
0.5
0.2
0.1
0.05
0.02
0.01
0.005
0.2
0.5
1.0
2.0
5.0
10
20
50
100
200
INTENSITY λ5577 (KILO-RAYLEIGHS)

Figure 11